01P-230

A Methodology to Simulate Piston Secondary Movement under Lubricated Contact Conditions

Günter Offner, Hubert M. Herbst, Hans H. Priebsch
Christian-Doppler Laboratory for Engine and Vehicle Acoustics at Institute for Combustion Engines and Thermodynamics, TU Graz, Austria and AVL List GmbH,Graz, Austria

ABSTRACT

The authors want to introduce a general methodology for the simulation of the dynamics of the piston-liner contact considering a realistic oil film at inner liner wall. Because of the complexity of this problem and in order to minimize computing time a twin model was developed. Firstly, a simplified model is used to compute piston motion trends and piston ring lubrication in minimum simulation time. Secondly a very detailed model simulating multi-body dynamics, surface vibrations and elasto-hydrodynamic contact is applied.
Both, the theoretical background of the twin model and the advantages of the coupled simulation procedure given in the wide range of considerable influences are discussed. The result examples focus on interaction effects of piston secondary movement and the influence of the available oil film. Finally, the status of verification of the models using measured results is shown.

INTRODUCTION

Beside the primary reciprocating motion, the piston performs a secondary motion (piston slap) due to the gap between piston and cylinder liner. Piston slap is an impact phenomenon causing engine noise and cavitation in the cooling water jacket. Well known as a possible problem for diesel engines, it can also be observed in modern gasoline engines. The phenomenon is known as a very significant source of noise excitation mainly in the 2 kHz octave band. Sliding contacts between piston skirt and liner also affect wear and the mechanical friction losses of the engine. Furthermore, in interaction with the piston rings, effects on blow-by and lube oil consumption can be observed. Therefore, the reduction of friction and wear due to the contact between piston and liner and the minimization of piston slap induced noise are main goals in the development of an internal combustion engine. This noise reduction is more often related to the avoidance of customer annoyance and subjective complaints than to meet legislation limits.
Piston-to-liner contact occurs directly between piston skirt and liner and indirectly via the piston rings. The structure in the contact area is excited radially in the piston slap direction, and tangentially in the sliding direction. The clearance between piston skirt and liner is determined by their shapes. Each shape results from the manufacturing profile and actual deformations due to loads (e.g. temperature, gas, assembly loads). Parts of the clearance are filled with oil. The amount of oil filling depends on the oil itself, on the contacting parts (piston, rings and liner) and the engine running conditions.

Hence, the typical effects in the piston-to-liner contact like combustion, structural dynamics, oil film behaviour, temperature and surface profiles of the components etc. are well known. But the effort to predict this contact within a simulation procedure becomes rather costly in CPU, as all relevant effects interact to one another and simplifications in the models may lead to wrong conclusions. Therefore, suitable and time saving representations of the effects in the simulation models must be central features in order to get valid and effective results.

For the detailed analyses of all important parameters concerned, a twin model has been developed by the authors. The total simulation process is divided into two parallel processes:

- A complex multi-body-system considering detailed elasto-hydrodynamic piston skirt lubrication (EHD-Piston) and
- a simplified multi-body-system with dry piston-to-liner contact (DRY-Piston).

The EHD-Piston model takes three-dimensional linear elastic body dynamics of all structural components into account. The piston-pin as well as the conrod can be represented via a beam-mass model alternatively. This alternative representation and the modeling of the component contacts depend on the application. In case of this piston-to-liner contact analysis, a full elasto-hydrodynamic representation is considered in the contact between piston skirt and liner. Forces both in the piston-pin bearings, and in conrod small-end bearings and in conrod big-end bearings are modeled using nonlinear functions.

Due to the complex structure of the EHD-Piston model, the simulation process is CPU-time intensive. In order to be able to perform trend calculations, the simplified DRY-Piston model has been developed. The components piston, piston-pin and conrod are represented by single mass models, the liner is a rigid body. For the computation of the dry piston-to-liner contact, the contact forces and moments cause radial deformations of the piston. Due to the rigid modeling, dynamical interactions with liner structure can not be considered in the dry contact calculation.

Because of the significantly reduced number of degrees of freedom, the DRY-Piston model is used in addition to the EHD-Piston model for the purpose of system parameter verifications. The model description for both EHD-Piston and DRY-Piston can be seen in Figure 2.

GOVERNING EQUATIONS

In the following section the formulation of representative equations, describing the mathematical models and the numerical solution strategies are described.

ELASTOHYDRODYNAMIC PISTON SKIRT LUBRICATION (EHD-PISTON)

For systematic approach the multi-body system has to be broken down into coupled systems, consisting of bodies, e.g. piston and liner, shaft and bearing, with linear elastic behaviour, plus connections, e.g. lubricated regions, considering the non-linear forces acting between the connected bodies. The basic equations used to simulate the elastic piston-liner contact are the

- Equation of motion to compute global motions and structural dynamics of bodies and
- Non-linear joint equations (e.g. Reynolds equation, spring-damper functions) to compute forces and moments acting between contacting bodies,

detailly discussed in [4].

Equation of motion for linear systems

In order to be able to calculate global motions and vibrations, the models of each component part have to be divided into a sufficiently high number of partial masses. The dynamic behaviour of each of these elastically connected rigid partial masses is given by the classical equation of motion for linear systems

$$\boldsymbol{M}\cdot\ddot{\boldsymbol{q}}+\boldsymbol{D}\cdot\dot{\boldsymbol{q}}+\boldsymbol{K}\cdot\boldsymbol{q}=\boldsymbol{f}^{(a)}+\boldsymbol{f}^{*}+\boldsymbol{p}^{*} \quad (1)$$

that can be derived from the equations of momentum and angular momentum. $\boldsymbol{M}$ and $\boldsymbol{K}$ denote mass and stiffness matrices, that are generated in a preprocessing step. $\boldsymbol{q}$ is the generalized displacement vector, consisting of translatorial and rotational motion components of the discrete partial masses. The damping matrices ($\boldsymbol{D}$) are calculated from given $\boldsymbol{M}$ and $\boldsymbol{K}$ according to Rayleighs method. The right hand side of the equation is given by a sum of force vectors. $\boldsymbol{f}^{(a)}$ and $\boldsymbol{f}^{*}$ are describing the external loads and the exciting joint forces and moments. External loads (e.g. gas force) are calculated from measurement data as functions of time. The non-linear terms of excitational forces and moments are resulting from joints, connecting one body to another (e.g. contact forces acting between piston and liner resulting from solution of Reynolds equation). In case of bodies with global motions (e.g. piston), non-linear inertia terms $\boldsymbol{p}^{*}$, discussed in detail in [6, 8], also have to be considered in the equation.

Both the big number of degrees of freedom of the connected bodies and the iterative scheme of the solution process, that will be described in a following section require a reduction of the number of degrees of freedom, [4] and [5]. The reduction (condensation) yields to the reduced equation of motion for linear systems

$$\overline{\boldsymbol{M}}\cdot\ddot{\boldsymbol{q}}_{a}+\overline{\boldsymbol{D}}\cdot\dot{\boldsymbol{q}}_{a}+\overline{\boldsymbol{K}}\cdot\boldsymbol{q}_{a}=\underbrace{\bar{\boldsymbol{f}}^{(a)}+\bar{\boldsymbol{f}}^{*}+\bar{\boldsymbol{p}}^{*}}_{\bar{\boldsymbol{f}}}, \quad (2)$$

where $\overline{\boldsymbol{M}}$, $\overline{\boldsymbol{D}}$ and $\overline{\boldsymbol{K}}$ denote the condensed structural matrices and $\bar{\boldsymbol{f}}$ is the condensed force vector. The reduced matrices together with the table of degrees of freedom and the geometry information are taken from FE software via an interface (For the results shown in this paper MSC-Nastran was used). Vibration analysis is performed on the reduced system only.

Non-linear joint equations - Reynolds equation

In order to be able to model the connections between contacting elastic components (main bearing, crank pin bearing, piston pin bearing or piston-liner contact) the resulting forces and moments have to be calculated. The detailed computing of these contact forces and moments for each engine cycle can be very time intensive. Therefore, the forces, in the crank pin bearing and the piston pin bearing are calculated according to the formula (3). Δx_i denotes the actual displacement, where $i=1,2,3$ correspond to the three directions of the coordinate system. The coefficients c_0, c_B, d_0 and d_B describe the nonlinearity of stiffness and damping related to a reference displacement x_B.

$$f_i=c_0\cdot\left(\frac{c_B}{c_0}\right)^{\left|\frac{\Delta x_i}{x_B}\right|}\cdot\Delta x_i+d_0\cdot\left(\frac{d_B}{d_0}\right)^{\left|\frac{\Delta x_i}{x_B}\right|}\cdot\Delta\dot{x}_i \quad (3)$$

Frictional moments are not considered in these joints. The pressure distribution of the oil film in the lubricated

region between piston skirt and liner is calculated using Reynolds equation derived from Navier-Stokes' equation and equation of continuity. The derivation takes as well laminar conditions, Newton fluid properties as special geometrical assumptions, like a constant oil film pressure in the direction of gap height into account. In order to get a time invariant (piston related) calculation region, the classical Reynolds equation, that is given in a space fixed coordinate system, is transformed into a piston fixed coordinate system, detailly discussed in [5]. The resulting equation is

$$\frac{\partial}{\partial x}\left(\frac{1}{12\overline{\eta}}\overline{\theta}\cdot\overline{h}^3\frac{\partial\overline{p}}{\partial x}\right)+\frac{\partial}{\partial\overline{z}}\left(\frac{1}{12\overline{\eta}}\overline{\theta}\cdot\overline{h}^3\frac{\partial\overline{p}}{\partial\overline{z}}\right)= \\ =\frac{-w_{Piston}+w_{Liner}}{2}\frac{\partial\left(\overline{h}\cdot\overline{\theta}\right)}{\partial\overline{z}}+\frac{\partial\left(\overline{h}\cdot\overline{\theta}\right)}{\partial t}. \quad (4)$$

The axial velocity components of both connected bodies, w_{Piston} and w_{Liner}, define the shear velocity part of the equation.

Coupling of equations

Equation (2) has to be solved in generalized condensed coordinates $\boldsymbol{q}_a$ for each body with known external forces, calculated excitation forces and moments and non-linear inertia terms. In order to calculate the positions of the partial masses, the equation of this body will be integrated. For the derivatives with respect to time of the generalized displacement vector, a direct implicit integration method is used ([1], [2], [5]). The resulting linear system is solved by factorization using the method of Cholesky, [1].

The excitation forces $\boldsymbol{f}^*$ needed for solving equation (2) are calculated from the contacts to other bodies. If the contact is modeled using a spring-damper function (main bearing, crank pin bearing, piston pin bearing or piston-liner contact), equation (3) yields the excitation forces for the corresponding degrees of freedom for both connected bodies. In the more detailed piston-liner contact, the components of $\boldsymbol{f}^*$ have to be calculated by integrating the oil film pressure in the clearance between the two connected bodies. The pressure distribution in the lubricated region, is calculated by solving the equation (4) in the piston fixed coordinate system. The oil viscosity η may be constant or it may depend on the oil film pressure. The calculation is performed on an equidistant calculation grid, moved with the piston skirt surface. Because of the regular structure of the grid nodes, a finite volume method is used for calculation. Both pressure distribution in the lubricated region and the contact region itself are determined iteratively. The classical SOR method (successive over relaxation) is used, considering a simple cavitation algorithm [5].

The condensed equation of motion (2) for each connected body and the equations computing the forces and moments acting between connected bodies, (3) and (4), are numerically coupled to a total system. Due to the non-linear characteristic of this system, it has to be solved in the time domain. In order to minimize numerical error, a direct implicit integration method (Newmarks method) considering adjusted time step size is used for time integration. In each time step both the equilibrium in the equation of motion and in Reynolds equation and the equilibrium of the total system have to be fulfilled. Figure 1 shows the interaction of excitation loads $\boldsymbol{f}^*$, resulting from integration of pressure distribution $\overline{p}(x,\overline{z})$, and the function of clearance height $\overline{h}(x,\overline{z})$ in the lubricated region between two connected bodies.

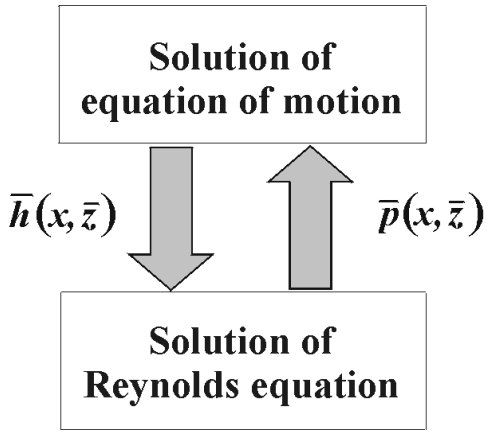

Figure 1: Interaction of the equation of motion and the Reynolds equation

MULTIBODY DYNAMIC SYSTEM WITH DRY PISTON LINER CONTACT (DRY-PISTON)

The equation of motion (1) is also applied on the individual components for the simplified model. The model components are given by the piston, pin, piston ring and con-rod. The secondary movement of the piston is predicted by degrees of freedom in axial, transversal and rotational direction. One transversal degree is added to the system of equations when the system is applied to an articulated piston. A rigid connection in both of the rod bearings is assumed and the crank pin should rotate with constant angular velocity. For the piston to liner contact an elastic solid-to-solid approach is used to determine side forces and moments as well. The nodal force on a surface grid on the piston is calculated by the formula (5) for those points having zero clearances

$$f_i=\sum_{j=1}^{N}K1_{ij}\,\delta_i+\sum_{j=1}^{N}K3_{ij}\,\delta_{ij}^3 \quad (5).$$

In this non-linear equation the coefficients K1 denotes the linear part of the radial piston stiffness and K3 the non-linear, respectively. The second term takes into account changes in the contact area, which are beyond the scope of the simulation grid. In particular, the coefficients for an individual piston are generated by using measured load deformation data or FE simulation. The interaction of friction for either mixed or hydrodynamic lubrication is determined according the law of Stribeck.

The entire simulation model includes predictions for axial piston ring motion, inter-ring pressure, oil film heights on liner wall and lube oil consumption, respectively. Within this model the problem of component dynamics and lubrication is split up into three individual simulation parts: piston secondary movement, piston ring dynamics and lube oil consumption. A description of the applied models, particularly, is presented in [3, 7]. However, in the current study the focus of attention is set on the left oil film by the ring package, which has also a substantial influence on the piston skirt lubrication. Additionally, it is worth mentioning whether a pre-calculation of the left oil film predicts the amount of oil, available for the piston skirt, sufficiently.

SIMULATION TECHNIQUES

The total simulation procedure consists of three main steps:

1. Preprocessing
2. Vibration analysis
3. Postprocessing

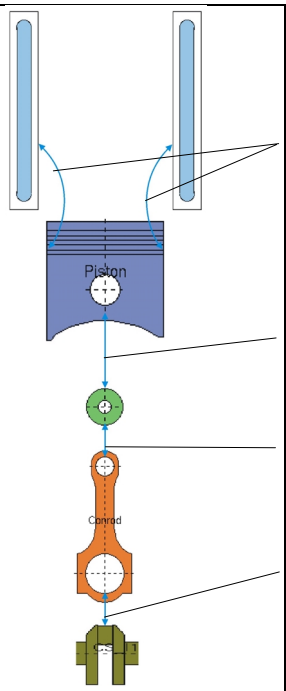

Component	DRY-PISTON	EHD-PISTON
Liner	Rigid body	Elastic (condensed FE model)
Piston/Liner Contact	Dry, Friction function	Elasto-hydrodynamic (EHD)
Piston	Single Mass /Moment of Inertia Radial elasticity	3D FE-Model condensed to surface nodes and modes
	3D Piston/Liner Profiles according machinery, temperature and assembly load	
Piston/Pin Bearing	Rigid, Friction function	Non-linear or EHD
Piston-Pin	Single Mass / Moment of Inertia	Beam/Mass or 3D Volumetric
Conrod Small-End Bearing	Rigid, Friction function	Non-linear or EHD
Conrod	Single Mass / Moment of Inertia	Beam/Mass or 3D Volumetric
Conrod Big-End Bearing	Rigid, Friction function Constant angular velocity	Non-linear or EHD
Crankshaft		Elastic (condensed FE model) Variable angular velocity

Figure 2: Model description for both EHD-Piston and DRY-Piston

The preprocessing step includes the generation of geometries and structural matrices for each elastic body using a normal FE-software package (for the analysis shown in this paper, MSC-Nastran was used). In order to enable an efficient solution of vibration equations, the EHD-Piston model uses a reduced (condensed) set of degrees of freedom. By doing this, the number of degrees of freedom of a piston can be reduced significantly (e.g. from 25000 to 700).

In case of the DRY-Piston model the contact stiffness coefficients are calculated via FE-simulation. The structural matrices together with the table of degrees of freedom and the node positions are taken from FE software via an interface. Furthermore, external loads and contact surface profile data for connected bodies are generated in the preprocessing step.

Neither the piston-liner nor the bearings have exact cylindrical contours (e.g. manufacturing profile of a piston skirt (Figure 3), deformation due to assembly and thermal load of a liner contact surface. Even if these deviations are in the range of a few microns, this fact has to be considered in the vibrational simulation process also. Inaccurate contact surface profiles can lead to systematic errors in the calculation, affecting the global motion as well as the vibrational motion results significantly. Due to this fact, both the EHD-Piston model and the DRY-Piston model consider contact surface

profiles, calculated from measured data using numerical interpolation with the highest possible accuracy.

The postprocessing step includes datarecovery of the calculated data to the uncondensed system (EHD-Piston model only) and detailed contact statistics.

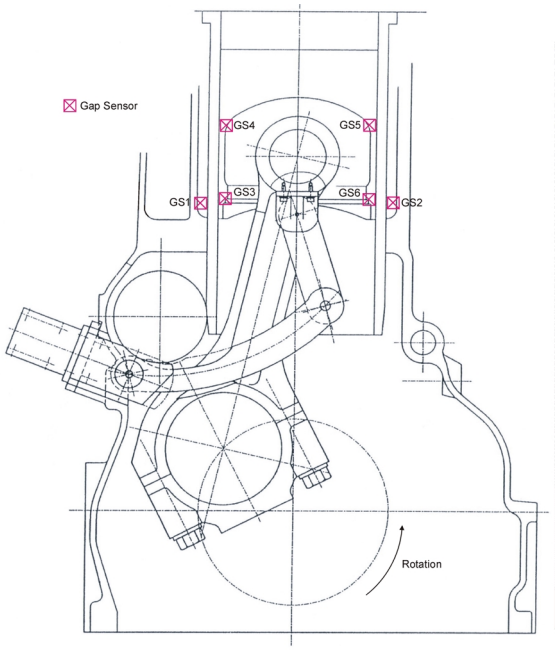

Figure 3 Piston and liner instrumentation

THEORETICAL RESULTS AND VERIFICATION WITH MEASUREMENT

TEST ENGINE AND MEASURING METHOD

The behavior of the piston secondary movement was investigated at a water cooled truck diesel engine with 2 liters/cylinder displacement and a maximum peak pressure of 115 bars at engine speed of 2000 rpm. The installed Aluminum mono-block piston, having a nominal diameter of 128mm, showed a piston pin offset of 1.3 mm to the minor side, which is known as a method to maintain the piston in upright position during the power stroke. In order to measure the piston movement over crank angle four gap sensors were attached in a cross sectional plane from the piston minor to major side. In addition two gap sensors were mounted in the liner at a height where the piston top land has its reversal point at bottom dead center. Figure 3 illustrates the location of all gap sensors and the linking device for the wire assembly.

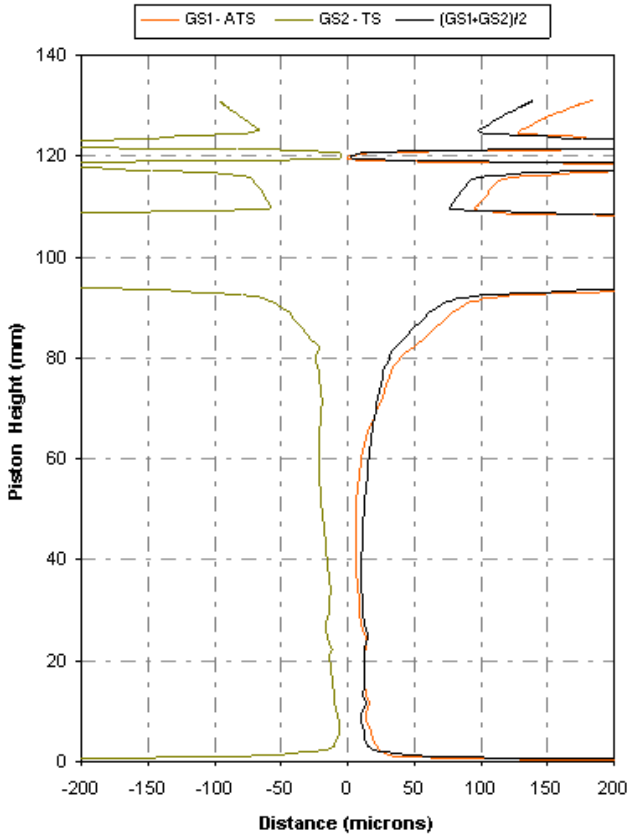

Figure 4 Piston to liner clearance over entire cycle, 800rpm – full load

DETERMINATION OF PISTON AND LINER PROFILE

Since the piston and liner are substantial deformed by thermal and assembly loads the profiles for piston and liner as well have been adjusted with the aid of the gap sensors signals. When the piston passes the sensors at the end of the intake stroke the piston side force is rather low. Therefore, the measured distances are mostly related to the geometric profile of the piston. Figure 4 shows the liner distances on piston minor and major side and the extracted profile. The spike at a position of 120 mm from the bottom end of the piston indicates the passing running face of the top ring which is surrounded by the piston top and second land. Applying the same procedure to the piston fixed sensor signals leads to the liner profile. Unfortunately, the signal of gap sensor 5 has already been lost at the very beginning. With increasing engine speed the second gap sensor on piston major side was also lost. At least the remaining data was sufficient enough for the determination of both profiles at 800rpm, full load and 2000 rpm, full load and quarter-load. Figure 5 shows the piston and liner profiles. Despite the initial piston to liner clearance of 150 microns the minimum clearance at piston top dead center position drops to a rather low value of about 6 microns diametrically. This is related to the cooling water jacket which maintains this zone at a lower temperature level. However, such a small clearance was only observed for intake and exhaust stroke. At crank angle

positions with high piston side forces both piston and liner deformation leads to a substantial increase in clearance.

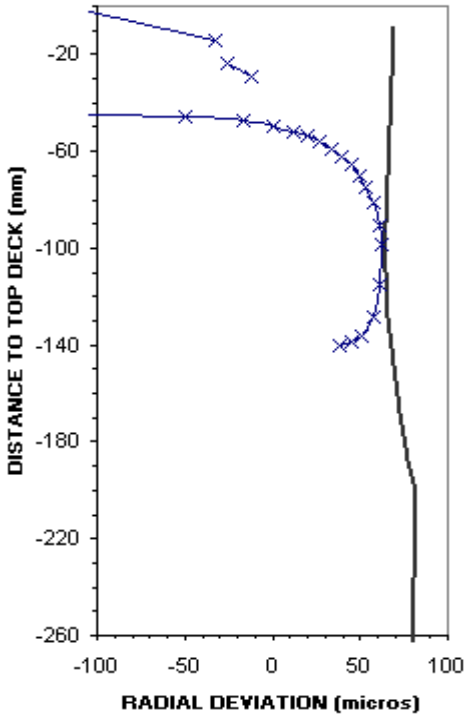

Figure 5 Interpolated piston and liner profile, 800rpm – full load

COMPARISON OF MEASURED AND PREDICTED PISTON SIDE CLEARANCES

In Figures 7 to 9 the comparison of both multi-body analysis and the measurement for the gap clearances on piston major and minor side is shown. The selection of the test cases was motivated by the intention in having cases at different piston side thrusts and piston speeds – 800 rpm at full load, 2200 rpm at 1/4 and full load. Those cases with higher side forces tend to lowest lubrication gaps shortly before and after firing top dead center (FTDC). On the other hand, the case with weakly loaded piston and high engine speed demonstrates the piston movement driven by inertia and hydrodynamic piston skirt forces. The validation of both methods is focused on the timing and the absolute course of the clearances around FTDC, firstly. Just then, when the piston changes its seating from the minor to the major side the tilting and the total side clearance has a significant impact on impulsivity and amplitude of the slap induced engine noise. Secondly, the overall tendency of the transverse movement is of great importance as soon as specific slap events are of interest apart from FTDC. At the end the development of clearances and relaxation of waviness over crank angle point out how well damping by lubrication is predicted. Even the last point allows an assessment of assumed and predicted amount of oil available for the piston skirt lubrication since the EHD-Piston model can handle partially flooded contact surfaces. The modelling of the elastic bodies in the EHD calculation uses both beam/mass and 3D volumetric elements (figure 2). In the following examples, the piston-pin as well as the conrod are modelled with beam/mass elements. Due to a reduced simulation time, the crankshaft is represented by one node moving along a circle with constant velocity.

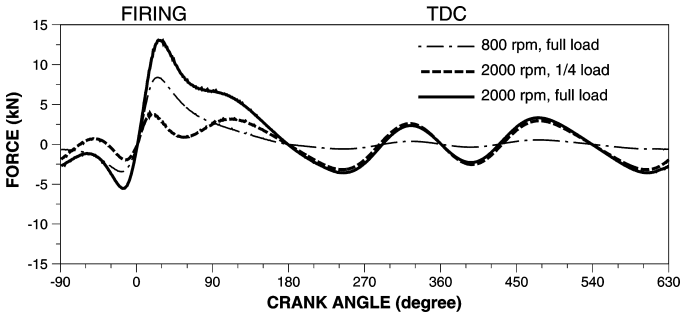

Figure 6 Lateral piston pin force at different engine operating conditions

As can be seen in Figure 7 the comparison between measurement and prediction various from extremely good to reasonably good. Within the period of compression the measured clearances at the lower end of the skirt (GS3 and GS6) show an amount of about 25 microns almost equal on both sides. When the piston decelerates around –58 degree crank angle (degCA) the signal GS4 closes shortly which indicates an inclination towards the liner wall on the minor side. At –30 degCA the inclination angle slightly reverses its direction as can be seen in the crossover of the minor side signals. With increasing minor thrust load the clearance at GS3 drops into ranges of 3 microns and lower in magnitude.

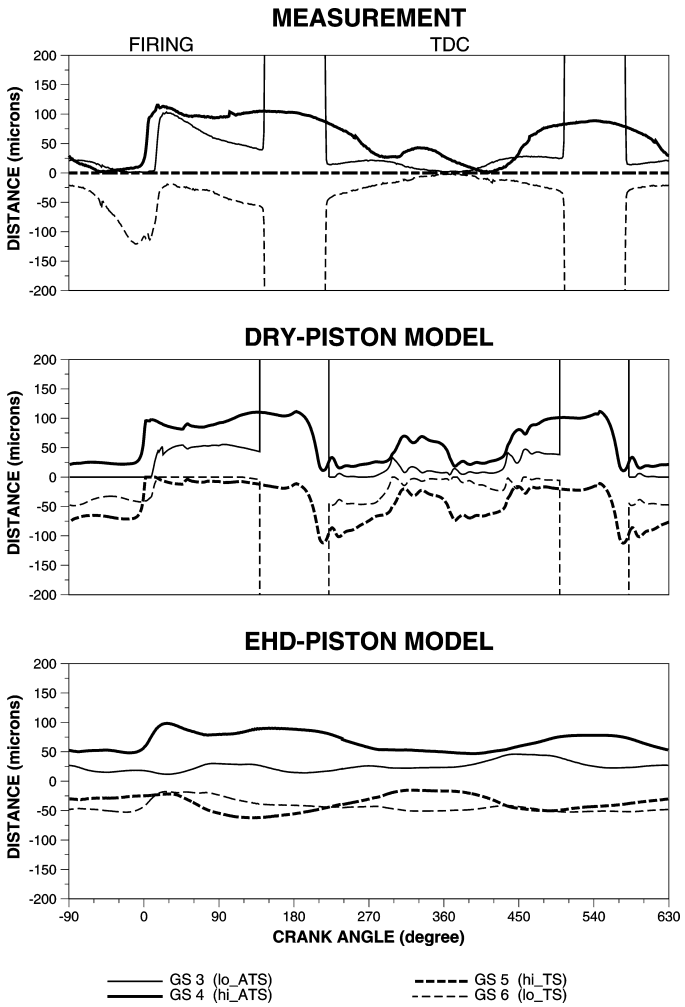

Figure 7 Comparison of predicted and measured piston side clearances at 800 rpm, full load

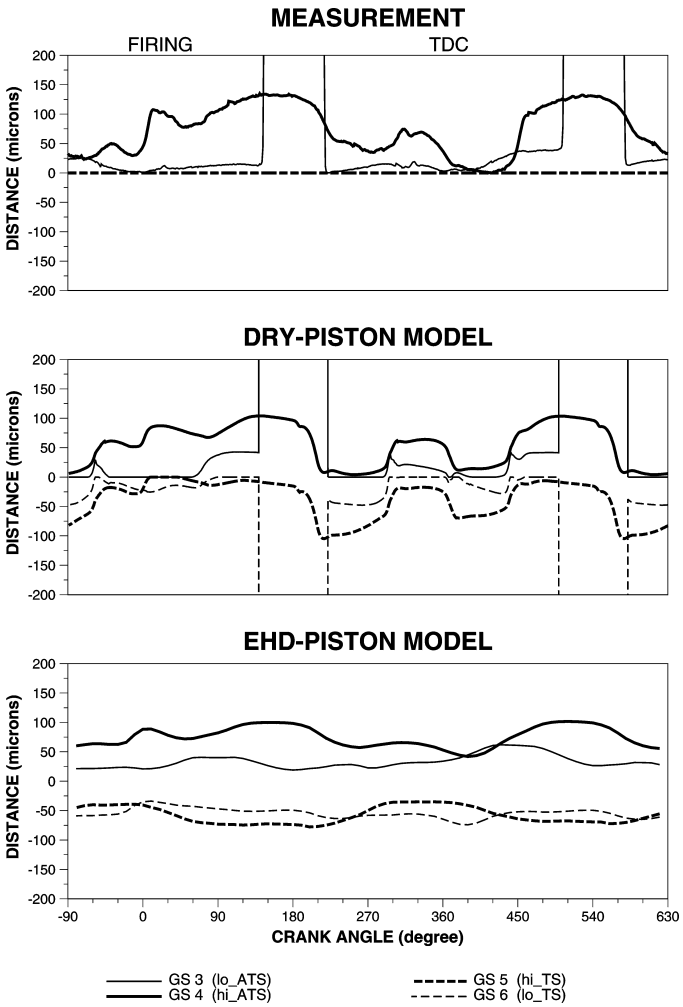

Figure 8 Comparison of predicted and measured piston side clearances at 2000 rpm, 1/4 load

Just before FTDC GS4 shows a remarkable increase which rings in the piston slap. With the crown part ahead the piston falls towards the major side followed by the skirt part which is a well known movement characteristic for such kind of pin offset. An excellent correlation in timing is achieved when a comparison is drawn between measurement and both predictions. At 5 degCA the error in the peak clearance at GS4 may result from some uncertainty of the liner profile there. However, the predicted clearances at lower skirt end with the dry model show a substantial deviation from the measurement. This can be traced back to the absence of the contribution due to the deformation by gas load. Such a contraction resulting in a V-shaped piston profile is missing in the current model. In case of the EHD-Piston model the lower skirt part remains in mid-position. Any attachment to either minor or major piston thrust side is prevented by the lubrication forces, which emphasize that the assumed oil amount of 80 microns is over-estimated. On the other hand, the DRY-Piston model leads to zero clearances. Even in piston positions with low lateral piston side forces as can be seen in Figure and 6 and 7.

The dry contact model does not generate any balancing force in this free-motion period. Also, the tilting and the change in clearance at GS4 from 180 to 270 degCA is over-predicted, which is related to the same matter and continues over intake to compression stroke.

For the examination of influences due to piston inertia forces at relatively intermediate gas loads, the contact analysis tracks the piston transverse movement predicted by both models as good as for 800 rpm – full load. In this case a specific feature is seen during compression stroke between –60 and –30 degCA, which was not observed in all other full load conditions. As a result of the inversion in thrust load (Figure 6) the piston is partially losing the contact on its minor side. The crown part is lifted off the liner wall and remains for about 20 degCA in this unstable thrust condition before it is slapped toward the liner as gas load is continuously increasing. However, an obvious lift is only predicted by the dry model. The clearance in the measurement develops to lower magnitudes in this period, which is basically related to the thermal contraction of the liner. Finally, the tracks of signal GS4 are qualitatively drawn very well by both models.

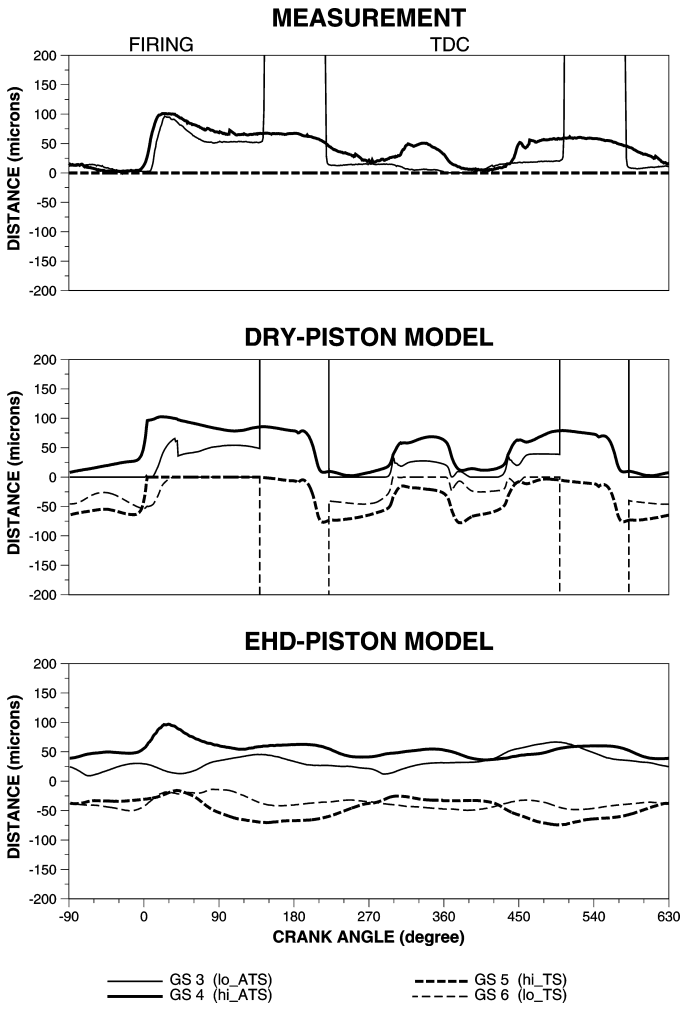

Figure 9 Comparison of predicted and measured piston side clearances at 2000 rpm, full load

The last case of our application study is almost identical with case - 800 rpm, full load. Unfortunately, the signal at piston major side GS6 was lost and therefore, any assignment of clearance change within FTDC to 140 degCA either to thermal liner expansion or to piston-liner deformation, forced by the gas load, is more speculative than fully known. Nevertheless, when focusing on timing around FTDC and development of the signals over the entire cycle it is seen that even at high engine speed and loads a pretty well correlation is achieved. Beyond that, the formation of clearance on piston minor side is much smaller for both signals this time when the piston enters the high compression zone at –30 degCA.

ASSESSMENT OF OIL FILM FORMATION FOR THE EHD-PISTON MODELL

The clearance between the two contacting surfaces at piston skirt and liner wall does not operate at fully flooded lubrication condition, rather a system with oil starvation has to be applied for the piston to liner contact. From this it follows, that damping effects on transverse movement, maximum peak pressure and slap distribution are highly influenced by the oil film thickness available as earlier studies [5] and other authors [9, 10] have already pointed out.

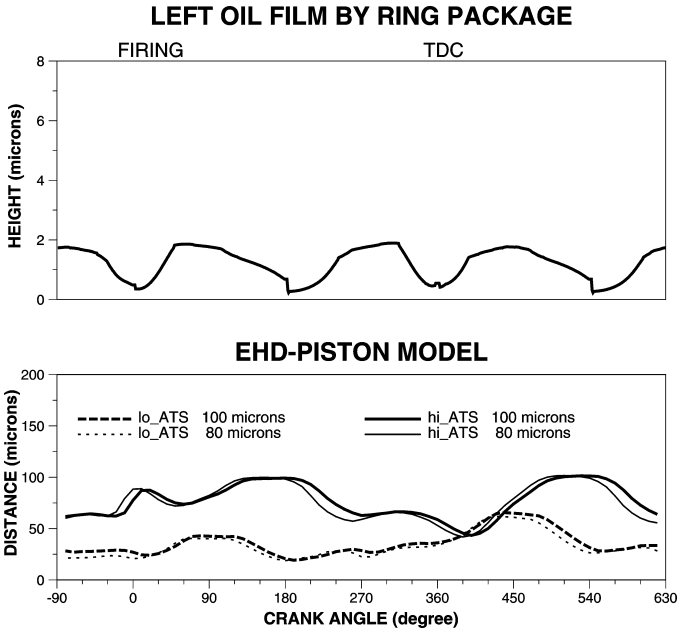

Figure 10: Comparison of left oil film thickness and piston gap distances at 2000 rpm, ¼ load

At that very moment when the piston changes its seating from minor to major thrust side around FTDC the assumed oil starvation will directly influence the predicted slap intensity. The assumption is still valid during field studies on piston design by simulation as long as the varied system parameter does not result in a substantial change on the oil film thickness. In order to have a more predictive simulation method, the results of a ring dynamic and lubrication simulation [3, 7] should be applied for determination of the available oil film thickness.

The top diagram in Figure 10 draws the left oil film on the liner wall left by the ring package. The amount of thickness changes from approximately 0.5 microns at FTDC to 1.9 microns at 40 degCA. Compared to the simulation with the EHD-Piston model the gap distance is about ten times higher, when a oil supply of 100 and 80 microns , respectively, is applied at the liner wall. In current state of the EHD model it was not possible to execute a simulation with a offer of oil below a heigth of 80 microns due to mixed lubrication contacts. Therefore, an approach to oil heights determined by the piston ring simulation was not attempted. However, the results of the DRY-Piston model (Figure 8) show a reasonably good correlation with the measurements which leads to the result that the oil height must be clearly below 80 microns.

CONCLUSION

Beside the theoretical background of both the elasto-hydrodynamic piston lubrication model and the multi-body dynamic model with dry piston to liner contact, the

simulation procedure is presented in this paper. The EHD model accounts partially flooded skirt lubrication. In addition the methodology of the so called twin model is introduced where in a first step the amount of liner lubrication is determined. In the second step predicted oil film thickness should feed the EHD piston skirt simulation. Furthermore, the time-saving simplified dry piston contact model is verified and the border of its applicability is determined. The summarized conclusions are as follows:

- The predicted secondary motion for both the EHD- and the DRY-Piston model varies from extremely good to reasonably good.

- The timing when the piston changes from minor to major thrust side at FTDC is excellent predicted by the DRY-Piston model. For the EHD model the damping due to lubrication is found being dominant in comparison to piston side force.

- In the crank angle range from exhaust stroke to intake stroke the results have a good correlation by means of transversal piston motion as well as absolute gap values. However, the secondary movement in the dry model simulation shows a sharply change of piston seating. This is traced back to the absence of any damping effects due to oil film lubrication.

- In order to achieve the low oil amount predicted by the piston ring simulation, an enhancement of the EHD model seems to be necessary.

ACKNOWLEDGMENTS

The work described within this paper was funded by the Austrian Government and by the AVL List GmbH, Graz, Austria. The measurements and the instrumentation of gap sensors were performed in co-operation with Federal-Mogul Burscheid GmbH.

REFERENCES

1. Bathe, K.-J.: *Finite-Elemente-Methoden*, Springer Verlag, 1990.
2. *Excite Reference Manual (Version 5.0)*, AVL LIST GmbH, Graz, 1999.
3. Herbst, M. H.; Priebsch, H. H.: Simulation of Piston Ring Dynamics and their Effect on Oil Consumption, SAE Paper 2000-01-0919.
4. Offner, G.; Krasser, J.; Laback O.; Priebsch H. H.: *Simulation of Multi-body Dynamics and Elastohydrodynamic Excitation in Engines Especially Considering Piston to Liner Contact*, ImechE, J. o. Multi-body Dynamics, Part K3, 2000.
5. Offner, G.; Priebsch, H. H.*: Elastic Body Contact Simulation for Predicting Piston Slap Induced Noise in IC Engines*, IMechE2nd Triennial Intern. Symposium Multi-body Dynamics, 2000.
6. Priebsch, H. H.; Affenzeller, J.; Kuipers, G.: *Prediction Technique of Vibration and Noise in Engines*, Proceeding, IMechE Conference Quiet Resolutions, 1990.
7. Priebsch, H. H.; Herbst, M. H.: Simulation of Effects of Piston Ring Parameters on Ring Movement, Friction, Blow-by and LOC, MTZ 60 (1999).
8. Priebsch, H. H.; Krasser, J.: *Simulation of Vibration and Structure Borne Noise of Engines – A Combined Technique of FEM and Multi Body Dynamics* to be published at CAD-FEM USERS' MEETING, Bad Neuenahr – Ahrweiler, 1998.
9. Ryan, P. R.; Wong, V. W.; and others: Engine Experiments on the Effects of Design and Operational Parameters on Piston Secondary Motion and Piston Slap, SAE Paper 940695, 1994.
10. Zhu, D.; Hu Y.; Cheng H. S.; Arai, T.; Hamai, K.: A Numerical Analysis for Piston Skirts in Mixed Lubrication - Part II: Deformation Considerations, Trans. of ASME, 1992.

CONTACT

Dr. Hans H. Priebsch is leader of the Christian-Doppler Laboratory for Engine and Vehicle Acoustics at the Institute for Combustion Engines and Thermodynamics, TU Graz, Austria and project manager for the software EXCITE of division Mechanical Systems/Advanced Simulation Technologies of AVL List GmbH, Graz, Austria

Günter Offner is research assistent of the Christian-Doppler Laboratory for Engine and Vehicle Acoustics at the Institute for Combustion Engines and Thermodynamics, TU Graz, Austria and developer of the software EXCITE of division Mechanical Systems/Advanced Simulation Technologies of AVL List GmbH, Graz, Austria

Hubert Maximilian Herbst is research assistent of the Christian-Doppler Laboratory for Engine and Vehicle Acoustics at the Institute for Combustion Engines and Thermodynamics, TU Graz, Austria and project manager for the software GLIDE of division Mechanical Systems/Advanced Simulation Technologies of AVL List GmbH, Graz, Austria

ABBREVIATIONS

$\boldsymbol{f}^{(a)}$ ……External loads

$\boldsymbol{f}^{*}$ ……Excitational loads

$\bar{\boldsymbol{f}}$ ……Condensed force vector

$\bar{h}$ ……Clearance height

$\bar{p}$ ……Oil film pressure

$\boldsymbol{p}^{*}$ ……Inertia terms

$\boldsymbol{q}$, $\boldsymbol{q}_a$ ……Generalized/condensed displacement vector

t ……Time
x ……Circumferential direction
y ……Gap direction
w_{Liner} ……Axial velocity of liner
w_{Piston} ……Axial velocity of piston
z ……Axial direction

$\boldsymbol{K}$, $\overline{\boldsymbol{K}}$ ……Stiffness matrices
$\boldsymbol{D}$, $\overline{\boldsymbol{D}}$ ……Damping matrices
$\boldsymbol{M}$, $\overline{\boldsymbol{M}}$ ……Mass matrices
$\overline{\eta}$ ……Lubricant viscosity
$\overline{\theta}$ ……Fill ratio